

Development and Characterization of Stretchable Conductive Composites for Sustainable and Energy-Efficient Electronic Applications

Mizah Ramli^{a,*}, Nur Hazwani Mokhtar^a, Mohd Nur Azmi Nordin^a, Mohamad Shukri Zakaria^a, Mariam Md Ghazaly^b, Mohd Haaziq Mohd Yusof^c

^aFaculty of Mechanical Technology and Engineering, Universiti Teknikal Malaysia Melaka, Hang Tuah Jaya, 76100 Durian Tunggal, Melaka, Malaysia

^bFaculty of Electrical Technology and Engineering, Universiti Teknikal Malaysia Melaka, Hang Tuah Jaya, 76100 Durian Tunggal, Melaka, Malaysia

^cFix & Go IT Specialist, Jalan Medan Pusat Bandar 7A, Seksyen 9, 43650 Bandar Baru Bangi, Selangor Darul Ehsan, Malaysia
 mizah@utem.edu.my

Stretchable conductive composite (SCC) has emerged as a promising material for flexible electronic applications. This study investigates the formulation, mechanical behaviors, and functional performance of SCC composed of graphene nanoplatelets (GNPs) and poly (3,4-ethylenedioxythiophene) polystyrene sulfonate (PEDOT:PSS), deposited on thermoplastic polyurethane (TPU). During the optimization of mixing parameters, three different configurations were studied: low-speed mixing at 400 rpm for 10 minutes, medium-speed mixing at 1500 rpm for 30 minutes, and high-speed mixing at 2000 rpm for 60 minutes. A mixing speed of 400 rpm for 10 minutes yielded the lowest sheet resistivity, indicating optimal dispersion. Surface treatments using methyl ethyl ketone (MEK) and an adhesion promoter significantly enhanced conductivity, suggesting improved film uniformity and filler–substrate interaction. Under cyclic loading at room temperature, 40 °C, and 80 °C, the SCC exhibited gradual changes in strain and resistivity. The optimized SCC with mixing parameter at 400 rpm for 10 minutes and coated with adhesion promoter showed the lowest sheet resistance of 3 Ω/sq. At 80 °C and after 30 cycles, the SCC displayed about a 3.8 % increase in strain capacity accompanied by higher resistivity that indicates reduced electrical stability. LEDs connected with SCC showed slightly lower brightness than those with wire connections at low voltages because of higher resistance. However, at 20 V they achieved a similar peak brightness (~41,000 cd/m²), demonstrating that SCC can work effectively as a flexible interconnect. This work demonstrates the feasibility of developing thermally stable SCC through optimized formulation and processing strategies.

1. Introduction

Recent advancements in electronics have emphasized not only enhancing device performance but also reducing size and improving flexibility to meet the demands of next-generation technologies. One promising innovation in this domain is the stretchable conductive composite (SCC), which combines electrical conductivity with mechanical flexibility, the key attributes for emerging applications such as wearable electronics, flexible sensors, and soft robotics (Liu et al., 2024). A wide range of conductive materials has been explored for SCC development, including metal-based composites, conductive polymers, and carbon-based materials (Jasmee et al., 2022). Carbon-based materials including fullerenes, carbon black, carbon nanohorns, carbon nanotubes (CNTs), and graphene have also been widely investigated. Graphene has gained significant attention as high-performance conductive fillers in SCC due to their unique combination of high aspect ratio, excellent electrical conductivity, and mechanical robustness (Liu and An, 2018). Recent studies have demonstrated the effectiveness of GNPs-based SCCs, which, when subjected to post-printing treatments such as thermal annealing and compression rolling, exhibit enhanced conductivity and mechanical durability (He et al., 2019).

The printed graphene patterns maintained a high conductivity of 8.81×10^4 S/m even after 1,000 bending cycles, with negligible performance degradation. Among conductive polymers, poly(3,4-ethylenedioxythiophene):poly(styrenesulfonate) (PEDOT:PSS) has garnered considerable interest due to its intrinsic conductivity, solution processability, and mechanical flexibility. PEDOT:PSS exhibits excellent film-forming properties, making it a suitable candidate for printable electronics. It can be further enhanced via post-treatment methods such as dimethyl sulfoxide (DMSO) or ethylene glycol (EG) doping to improve its conductivity. Its compatibility with various substrates and ability to maintain electrical performance under mechanical deformation make it a valuable binder and co-conductive component in SCC formulations. Studies have shown that PEDOT:PSS contributes not only to electrical performance but also acts as a flexible binder that improves strain tolerance in composite systems (Aleksandrova et al., 2024). Among available substrates, thermoplastic polyurethane (TPU) has gained significant attention due to its excellent elasticity, thermal stability, and compatibility with flexible electronics (Azlan et al., 2024). TPU can withstand strain rates up to 1000 %, making it a versatile material for various applications (Xiang et al., 2019). To meet growing industrial demands, high performance SCC must offer high flexibility, strong adhesion, thermal stability, and ease of processing at low cost. However, many existing formulations struggle to maintain conductivity and mechanical integrity under thermal stress. In particular, performance degradation at elevated temperatures remains a key challenge.

The sustainability and energy efficiency of the developed SCC can be explained through three aspects: low-temperature processing, low operational energy, and reduced metal usage. Curing the SCC at 60 °C requires significantly less energy compared with conventional or metallic-filler SCCs, which often need curing conditions of 100–200 °C. The developed SCC was capable of illuminating LEDs at low voltages, demonstrating energy-saving performance. Furthermore, the use of carbon-based interconnects in the SCC reduces the reliance on metallic fillers, which are resource-intensive and associated with high energy costs during extraction as well as environmental concerns. Although the use of PEDOT:PSS, solvent doping (DMSO, EG), surfactant-assisted dispersion (Triton X-100), and graphene fillers has been reported individually in earlier studies, their systematic integration, combined with TPU surface treatment, has not been fully explored. To clarify the incremental contributions of this work, a comparative summary is provided in Table 1, highlighting the differences between prior approaches and the present study. Therefore, this study investigates the thermal and mechanical performance of carbon-based SCC applied to TPU substrates, aiming to evaluate their conductivity, structural stability, and flexibility under various thermal conditions. These findings will contribute to the development of thermally stable, high-performance SCC tailored for future applications in flexible electronics.

Table 1: Comparison of prior conductive composite approaches with the present study

| Reference | Composition | Processing / Additives | Substrate | Deposition method | Limitation Compared to Present Work |
|---------------------------|---|--|---|-------------------|--|
| Aleksandrova et al., 2024 | PEDOT:PSS/graphene | DMF Solvent | PET | Spray | Flexible but not stretchable substrates. Cyclic loading in different humidity condition only |
| Kumar et al., 2022 | RTV-silicone rubber + GNPs + electrolyte iron particles | CAT-RM Vulcanizing Agent | - | Mold | Mechanical testing at room temperature only |
| Kishi et al., 2018 | PEDOT:PSS + Ionic Surfactant | Sodium Dodecyl Sulfate (SDS) or Sodium Dodecylbenzene Ionic Surfactant | PET, Pyrex glass and soda-lime glass substrates | Spin coating | Measurement of thermoelectric and wettability properties without mechanical testing |
| Zhang et al., 2021 | Polydimethylsiloxane (PDMS) + Graphite-welded CNTs | High temperature annealing (3000 °C) | PDMS | Infiltrate PDMS | Investigation on cyclic testing without temperature variation |
| This Work | PEDOT:PSS + GNPs + DMSO/EG + Triton X-100 | Optimized mixing + MEK/adhesion promoter treated TPU | TPU | Screen Printing | Optimized composition with surface-treated substrate, tested under cyclic temperature conditions |

2. Methodology

2.1 Materials

The SCC was formulated using a conductive filler, a conductive polymer binder, and a multi-component solvent system. All chemicals were purchased from Sigma-Aldrich. GNPs of average lateral size 15 μm with surface area of 120 - 150 m^2/g and average thickness 6 – 8 nm was utilized. As the conductive polymer binder, 1.3 wt.% of poly(3,4-ethylenedioxythiophene):polystyrene sulfonate (PEDOT:PSS) dispersed in deionized water was employed. A ternary solvent system consisting of DMSO, EG, and Triton X-100 was employed to adjust the rheological properties and improve dispersion, with each component contributing to enhanced conductivity, film uniformity, and wetting behavior. For surface treatment, MEK purchased from Sigma Aldrich and commercially available adhesion promoter, Anchor Spray Paint (ASP) from DPI Holdings Berhad were used.

2.2 Fabrication of specimens

For the mixing process of SCC, three mixing parameter ranges were employed in this study: 400 rpm for 10 minutes, 1500 rpm for 30 minutes, and 2000 rpm for 60 minutes. GNPs were incorporated into the polymer binder and solvent mixture prior to the mixing process, which was carried out using a centrifugal mixer. The formulated SCC was subsequently deposited onto thermoplastic polyurethane (TPU) substrate using the screen-printing technique. This method involved the preparation of a stencil—serving as a patterned template with defined apertures that allow the liquid to pass through and form a design on the substrate surface. Prior to the screen-printing process, TPU substrates were treated by cleaning with MEK and adhesion promoters and then left to dry at room temperature. The SCC was deposited through the stencil openings, producing the desired pattern. Due to the low viscosity of the SCC, the doctor-blading method was employed during deposition to ensure even distribution across the stencil apertures. Doctor blading is widely used in industries such as electronics, solar cells, and battery manufacturing for producing uniform thin films on various substrates. The printed specimens underwent a curing process at 60 $^{\circ}\text{C}$ for 15 minutes. For further investigation of mechanical behavior and LED lighting prototype, the optimal mixing parameters and surface treatment that yielded the lowest resistivity were used in the specimen fabrication.

2.3 Resistivity Test

The electrical resistivity of the printed specimens was measured at room temperature using a four-point probe system (Jandel CYL-RM3000) with 1 mm probe spacing. A constant current was applied through the two outer probes, and the resulting voltage drop was measured across the two inner probes. This method was chosen to minimize contact resistance errors, ensuring an accurate characterization of the material's intrinsic resistivity.

2.4 Cyclic Loading Test

To evaluate the durability and performance of the SCC, cyclic mechanical loading tests were conducted using a custom-built mini tensile testing machine. This test was designed to replicate the operational environment of flexible and wearable electronics, where materials are regularly subjected to repetitive deformation such as stretching and bending, often in elevated temperature conditions. The SCC specimens had dimensions of 70 mm in length, 30 mm in width, and 0.05 mm in thickness, as shown in Figure 1a, with the thickness controlled using scotch tape as a spacer. The specimens were clamped onto the tensile fixture and subjected to uniaxial cyclic stretching with controlled displacement. During cyclic testing, one cycle corresponded to 5 s with 0.3 % elongation from the original length. The crosshead speed was set to 0.0315 mm/s, and the strain was calculated as the ratio of the elongation (change in length) to the original length. Testing was performed at three different cycle counts: 10, 20, and 30 cycles, representing light to moderate mechanical fatigue scenarios. To assess thermal influence on mechanical stability, the tests were conducted at three temperature settings: ambient room temperature (~ 25 $^{\circ}\text{C}$), moderate heating at 40 $^{\circ}\text{C}$, and elevated thermal conditions at 80 $^{\circ}\text{C}$. Each test was repeated three times. A precision thermal chamber integrated with the tensile setup was used to maintain stable temperature during testing. The mechanical response was recorded for each condition to analyze changes in mechanical integrity and correlate with electrical performance.

2.5 LED lighting prototype

In the final phase, the developed SCC was integrated into a prototype to evaluate its potential for automotive lighting. SCC circuits were printed directly onto TPU substrates to create flexible and stretchable conductive paths. Light-emitting diode (LED) was attached using conductive tape to maintain reliable contact without damaging the substrate as shown in Figure 1b. A conventional wire-connected LED circuit was used for comparison (Figure 1c). Luminance performance was measured under controlled conditions using a black-box setup at varying input voltages and observation distances by using a digital lux meter.

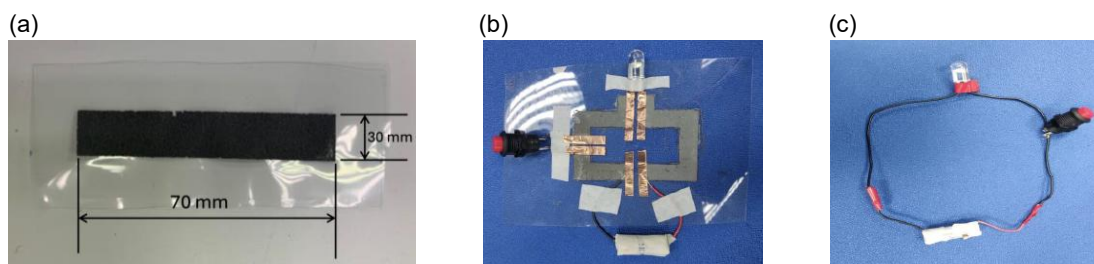


Figure 1: (a) SCC specimen for cyclic loading test, (b) LED connected with SCC on TPU substrate, and (c) LED connected with conventional wire

3. Results and Discussions

3.1 Optimization of mixing parameters

There were three samples fabricated for each mixing condition to measure the resistivity of SCC. Sheet resistivity measurement was performed at four different point in each sample as shown in Figure 2a. A total of 12 resistivity measurements were collected as shown in Figure 2b and 2c. Referring to Figure 2b, among the three tested mixing conditions, specimens fabricated at 400 rpm for 10 minutes consistently demonstrated the lowest sheet resistivity, averaging approximately $3.5 \Omega/\text{sq}$ across all samples. Furthermore, it has the most consistent data from all measurements. This result indicates superior electrical performance, and the GNPs disperse uniformly in the polymer binder. In contrast, samples processed at 2000 rpm for 60 minutes and 1500 rpm for 30 minutes exhibited higher resistivity values with fluctuating results. These findings indicate that lower-speed, shorter-duration mixing can produce more stable electrically conductive SCC than higher-speed, prolonged processing. Lower mixing energy allows the polymer binder (PEDOT:PSS) to interact more gently with the graphene surfaces, leading to better interfacial contact and improved charge transfer efficiency. Overly aggressive mixing may cause structural defects in graphene and agglomeration occurs due to van der Waals forces when graphene layers are excessively exfoliated or reduced in size. The investigation on surface treatment of substrates was performed by applying MEK and commercially available adhesion promoter to the substrates prior to screen-printing process. The best mixing parameter of 400 rpm for 10 minutes was applied. Figure 2c shows the comparison of resistivity results for three types of specimens. Specimens treated with MEK and adhesion promoter consistently exhibited lower sheet resistivity values across all measurement points around $2 \Omega/\text{sq}$. In contrast, the non-adhesion promoter condition showed higher initial resistivity. This trend suggests that untreated surfaces may initially hinder conductivity due to poor SCC formation or surface irregularities. Surface treatment with MEK or adhesion promoter improves the surface wettability, allowing the SCC to spread evenly. More uniform interfacial bonding between the SCC and the substrate reduces micro voids or cracks, leading to a more continuous path for the fillers to transport electrons. The superior performance of MEK and adhesion promoter treatments highlights the importance of surface preparation in achieving optimal electrical properties. These treatments enhance cleanliness, promoting better adhesion and uniformity, which in turn lower resistivity.

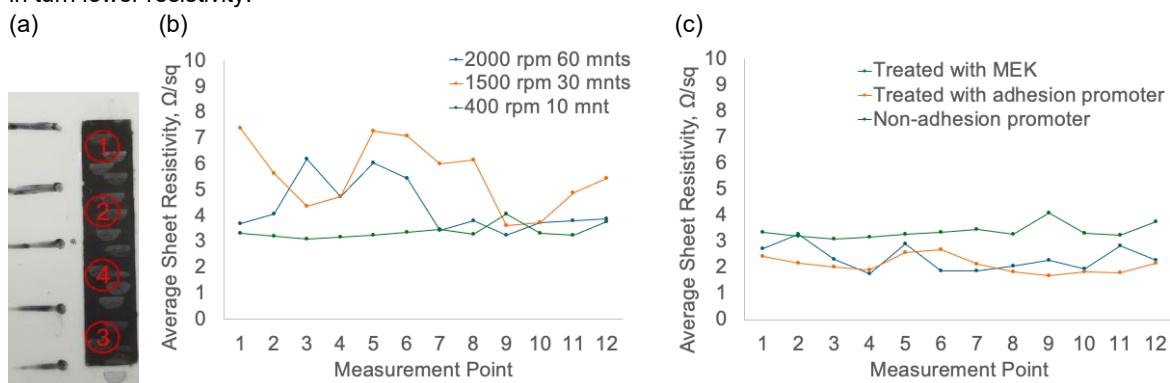


Figure 2: (a) Visual representation of the four measurement points used on each printed sample, (b) Sheet resistivity dependence on the mixing speed used for the SCC preparation. (c) Sheet resistivity results following different substrate surface treatments prior to screen-printing

3.2 Cyclic Loading Effect

Figure 3 presents the strain and resistivity results of SCC at three different temperatures after 10, 20, and 30 cycles of loading. The strain rate applied was 0.0315 m/s, with each cycle lasting 5 seconds. Across the datasets, a consistent trend is observed where strain and resistivity increase with temperature, indicating a thermally induced enhancement in material deformation. Figure 3a shows the strain percentage increases with both temperature and the number of loading cycles. At elevated temperatures (80°C), the material polymer chains or microstructures gain kinetic energy, weakening intermolecular interactions, which in turn develop higher strain percentage compared with lower temperature (40°C and room temperature). Due to repeated cycles of loading, repeated deformation occurs leading to microstructural fatigue, plastic deformation, and stress softening, which contribute to the increased strain percentage. In Figure 3b, the resistivity measurements are recorded for the same condition and cyclic loading. A clear trend is observed across the three datasets showing that resistivity increases with temperature and cycles of loading. Elevated temperatures increase atomic vibrations, making it harder for electrons to move freely. This reduced mobility increases the material resistivity. Under repeated cycles of loading, the recurrent strain may cause microcracks, filler displacement, or interfacial debonding between the conductive fillers and the polymer binder. These microstructural changes interrupt the percolation pathways that facilitate electron transport, resulting in increased electrical resistance.

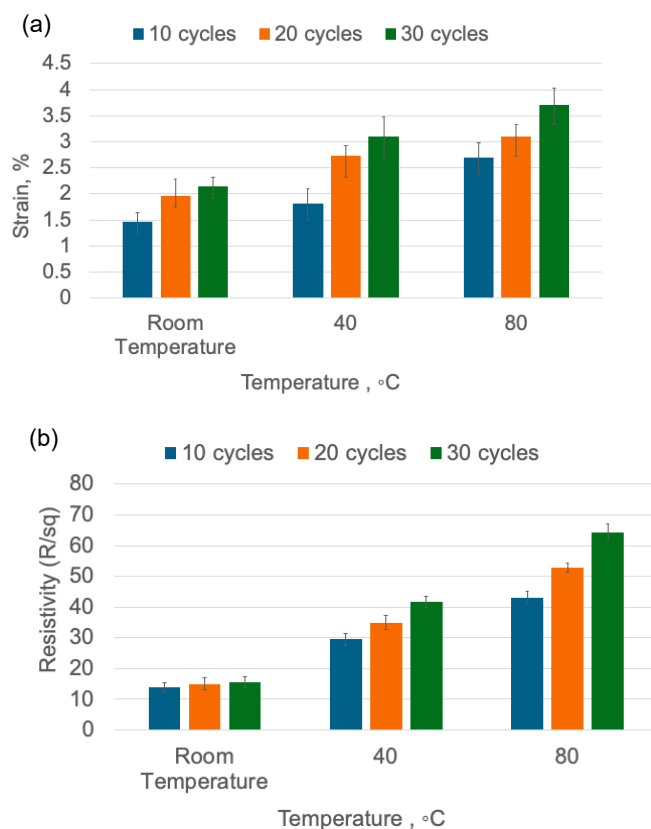


Figure 3: (a) Strain measurement, and (b) resistivity measurement of specimens under three environmental conditions for 10, 20, and 30 cycles of loading

Figure 4 illustrates the voltage-luminance characteristics of LEDs connected via conventional wire and SCC. Both conditions show a positive correlation between voltage and luminance, with wire-connected LEDs reaching a peak luminance of approximately 43,000 cd/m² at 20 V, while SCC-connected LEDs achieve around 41,000 cd/m². Wire connections offer lower resistance, allowing more current to flow and resulting in higher luminance. SCC, however, may introduce additional contact resistance or interface limitations due to its composite or printed nature. Although wire connections exhibit slightly superior performance at higher voltages, SCC demonstrates a stable and responsive luminance output across the voltage range, indicating its strong potential as an alternative to traditional wiring. With further optimization in improving conductivity, refining interface design, or incorporating conductive nanomaterials, SCC could effectively replace conventional wire circuits, especially in environments where mechanical flexibility and lightweight design are critical.

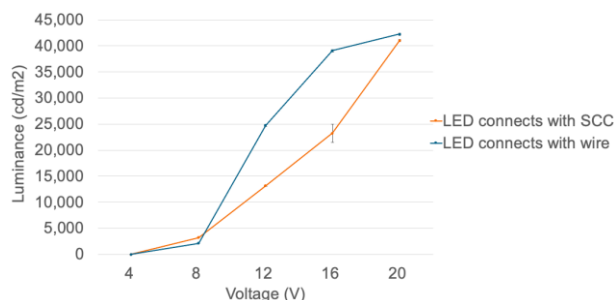


Figure 4: Comparison of voltage-luminance characteristics of LEDs connected via conventional wire and SCC

4. Conclusions

This study presents the formulation and characterization of a SCC composed of GNPs and PEDOT:PSS deposited on TPU substrate. The processing parameters were found to significantly influence filler dispersion and electrical behavior, with optimal performance achieved at a mixing speed of 400 rpm for 10 minutes, yielding the lowest and most stable sheet resistivity. Surface modification using MEK and adhesion promoters further enhanced conductivity by improving interfacial bonding. Cyclic loading tests at room temperature, 40°C, and 80°C showed that while resistivity increased with thermal exposure due to disruptions in conductive pathways, the SCC maintained stable performance under moderate deformation. Its potential was confirmed by integrating it into a flexible LED prototype, demonstrating its feasibility for lightweight, sustainable automotive electronics. Despite slightly lower luminance than wired LEDs, the SCC circuit's consistent functionality highlights its promise for next-generation flexible devices.

Acknowledgments

The authors would like to express gratitude to Universiti Teknikal Malaysia Melaka under grant no. PJPC/2024/FTKM-CARE/SC0018, and Advanced Material Characterization Laboratory (AMCHAL) for making this study possible.

References

- Aleksandrova M., Mateev V., Iliev I., 2024, Behavior of Polymer Electrode PEDOT:PSS/Graphene on Flexible Substrate for Wearable Biosensor at Different Loading Modes, *Nanomaterials*, 14(16), 1357.
- Azlan D., Ramli M., Zakaria M.S.B., Omar G.B., Dziaudin A.F.B., 2024, Validation of Thermoplastic Urethane Substrates for Stretchable Circuits: Experimental and Simulation Approach, *Proceedings of the 9th International Conference and Exhibition on Sustainable Energy and Advanced Materials (ICE-SEAM 2023)*, Lecture Notes in Mechanical Engineering, Springer, Singapore., 413–417.
- He P., Cao J., Ding H., Liu C., Neilson J., Li Z., Kinloch I.A., Derby B., 2019, Screen-Printing of a Highly Conductive Graphene Ink for Flexible Printed Electronics, *ACS Applied Materials and Interfaces*, 11(35), 32225–32234.
- Jasmee S., Ramli M., Othaman S.S., Omar G., 2022, Thermal Conductivity and Shear Strength Characterisation of Hybrid GNPs and Silane Functionalised BN as Thermal Conductive Adhesive, *The Journal of Adhesion*, 99(10), 1695–1743.
- Kishi N., Kondo Y., Kunieda H., Hibi S., Sawada Y., 2018, Enhancement of Thermoelectric Properties of PEDOT:PSS Thin Films by Addition of Anionic Surfactants, *Journal of Material Science: Materials in Electronics*, 29, 4030–4034.
- Liu J. and An L., 2018, Synthesis and Properties of Graphene/Carbon Nanotube/Epoxy Resin Composites, *Chemical Engineering Transactions*, 71, 949–954.
- Liu K., Duan T., Zhang F., Tian X., Li H., Feng M., Wang R., Jiang B., Zhang K., 2024, Flexible Electrode Materials for Emerging Electronics: Materials, Fabrication and Applications, *Journal of Materials Chemistry A*, 12(32), 20606–20637.
- Xiang D., Zhang X., Li Y., Harkin-Jones E., Zheng Y., Wang L., Zhao C., Wang P., 2019, Enhanced Performance of 3D Printed Highly Elastic Strain Sensors of Carbon Nanotube/Thermoplastic Polyurethane Nanocomposites via Non-Covalent Interactions, *Composites Part B: Engineering*, 176, 107250.
- Zhang F., Ren D., Huang L., Zhang Y., Sun Y., Liu D., Zhang Q., Feng W., Zheng Q. B., 2021, 3D Interconnected Conductive Graphite Nanoplatelet Welded Carbon Nanotube Networks for Stretchable Conductors, *Advance Functional Materials*, 31, 2107082.